Multiple lensing of CMB anisotropies

G. Fabbian
International School for Advanced Studies (SISSA), Trieste 34014, Italy

We study the gravitational lensing effect on the anisotropies of the Cosmic Microwave Background (CMB) performing a ray-tracing of its photons through intervening large-scale structures (LSS) distribution predicted by N-Body numerical simulations. We discuss differences of CMB lensing observables derived with this method with respect to the standard techniques usually employed in this context that are based on the Born approximation. Finally we analyze the impact of second order lensing effects propagating the full lensing jacobian through cosmic structures.

1 Introduction

The CMB is now firmly established as one of the most important cosmological probe thanks to the accuracy of the measurements of the recent Planck satellite and the current generation of suborbital CMB polarization experiments. In parallel to the studies on the primordial signal for cosmological applications, the attention of the community has swiftly moved towards the weak gravitational lensing of CMB anisotropies. Being sensitive to the whole matter distribution along the line of sight, CMB lensing can be used to infer information about the Large Scale Structure (LSS) distribution and on the parameters that govern the physics of structure formation at intermediate and late time (like, e.g., the dark energy and massive neutrinos properties).

2 Mathematical formalism

In weak lensing calculations, the effect of deflections of photons along the entire line of sight is described by the lens equation, which maps the final position $(\boldsymbol{\beta}, \chi)$ of the photon to the position of its source $\boldsymbol{\theta}$, i.e.

$$\beta_i(\boldsymbol{\theta}, \chi) = \theta_i - \frac{2}{c^2} \int_0^\chi \frac{(\chi - \chi')}{\chi\chi'} \Phi_{,\beta_i} \left(\boldsymbol{\beta}(\boldsymbol{\theta}, \chi'), \chi'\right) \mathrm{d}\chi', \tag{1}$$

where $\Phi(\boldsymbol{\beta}, \chi)$ is a gravitational potential and $\Phi_{,\beta_i}$ its spatial derivative. The relative position of nearby light rays is described by the derivative of the previous equation (lensing jacobian):

$$A_{ij}(\boldsymbol{\theta}, \chi) = \partial_j \beta_i(\boldsymbol{\theta}, \chi) = \delta^K_{ij} - \frac{2}{c^2} \int_0^\chi \frac{f_K(\chi - \chi')}{f_K(\chi) f_K(\chi')} \Phi_{,\beta_i \beta_k} \left(\boldsymbol{\beta}(\boldsymbol{\theta}, \chi'), \chi'\right) A_{kj}(\boldsymbol{\theta}, \chi') \mathrm{d}\chi'. \quad (2)$$

A is usually decomposed into four fields describing how the source at $\chi \equiv \chi_s$ is transformed by its interaction with the matter distribution,

$$A_{ij} = \begin{pmatrix} 1 - \kappa - \gamma_1 & -\gamma_2 + \omega \\ -\gamma_2 - \omega & 1 - \kappa + \gamma_1 \end{pmatrix}, \quad (3)$$

$\kappa(\boldsymbol{\theta}, \chi_s)$ describes image magnification, $\omega(\boldsymbol{\theta}, \chi_s)$ the image rotation while $\gamma(\boldsymbol{\theta}, \chi_s) = \gamma_1(\boldsymbol{\theta}, \chi_s) + i\gamma_2(\boldsymbol{\theta}, \chi_s)$ defines the complex spin-2 shear. The latter describes the shearing of the image, and can be decomposed into E and B-modes in analogy with CMB polarization. In the context of CMB lensing, the lens equation is usually integrated in the Born approximation, i.e. over the unperturbed, unlensed photon paths $(\boldsymbol{\theta}, \chi)$ [a]. Shear B-modes and image rotation are non-zero only if we take into account the full non-linear equation or the coupling between lenses at two different redshifts while are zero in the Born approximation.The overall effect of lensing deflection field can be expressed an effective deflection (vector) field that can be decomposed in a pure gradient of a scalar potential ψ (lensing potential), and a curl-like potential Ω:

$$\boldsymbol{\beta}(\boldsymbol{\theta}, \chi_s) = \boldsymbol{\theta} - \nabla\psi(\boldsymbol{\theta}, \chi_s) - \nabla \times \Omega(\boldsymbol{\theta}, \chi_s), \quad (4)$$

The latter is null in the Born approximation. The exponentially growing quality of CMB observations requires a great effort to simulate and make predictions for the various lensing observables with the highest possible accuracy. One of the major challenges lies in the improvement in the modeling of the LSS distribution to include the non-linear evolution of the dark matter distribution at low redshift as well as to include the multiple deflection of photons along the line of sight. We tried to overcome these last points at the same time implementing a multiple-lens plane (hereafter ML) method first sketched by Das & Bode [3].

3 From particles to surface mass density maps

Starting from an N-Body simulation, we create 3D simulated matter distribution around a chosen observer along the past lightcone. For this work we used the CoDECS [5] and DEMNUni [6] ΛCDM simulations. We overcome the problem of the finite volume of the simulation using box replication and randomization techniques. We then divided the lightcone in shell of $150h^{-1}$Mpc thickness and project all the matter particle inside a given shell over a single 2D spherical map. For each of these surface mass density map at different redshift we then solved the full-sky Poisson equation in the harmonic domain up to a given angular scale ℓ^ψ_{max} and extracted the lensing potential of each shell $\psi^{(k)}$ (see fig. 2). We also computed the effective integrated potential combining the single 2D mass maps with a proper lensing weight. To test that the box replication and randomization procedure did not create spurious effect, we checked that the total mass in each slice was consistent with the amount of mass expected from the cosmology of the N-body simulation. We found that this number agrees with theoretical expectation at sub-percent level at $z > 0.5$ and better than 2% level at $z \lesssim 0.5$ for the CoDECS simulation and is always sub-percent for the DEMNUni simulation. For both simulations we also found that the 1-point PDF of the surface mass density planes is well described by a modified log-normal distribution following the Das & Ostriker [9] model in agreement with previous numerical results.

[a] this is equivalent to drop the dependence over the lensed position $\boldsymbol{\beta}$ in eqs. (1, 2) and replace it with $\boldsymbol{\theta}$.

4 Lensing the CMB

To lens the CMB we first generated a gaussian realization of the unlensed CMB up to a given scale ℓ_{max}^{CMB}. To propagate the CMB photons through the different shells we used the the publicly available code Lenspix. Starting from the $\psi_{\ell m}^{(k)}$ coefficients, we computed the deflection field for each shell $\boldsymbol{\alpha}^{(k)}$ in the harmonic domain[b]. We then assumed that the Born approximation is valid between two consecutive shells. Each time a CMB photon crosses a mass shell in the direction $\hat{\mathbf{n}}^{(k)}$, is remapped into $\hat{\mathbf{n}}'^{(k)}$,

$$\hat{\mathbf{n}}'^{(k)} = \hat{\mathbf{n}}^{(k-1)} + \boldsymbol{\alpha}^{(k)}, \tag{5}$$

where $\hat{\mathbf{n}}^{(k-1)}$ represents the unlensed position of the CMB photons at the previous step. Pixel based method are affected by several numerical effects[2] and therefore we tested the convergence of our results with respect to choices of spatial resolution and cut-off in power in the Fourier domain used to synthesize signals on the sphere (i.e. $\ell_{max}^{CMB}, \ell_{max}^{\psi}$). The baseline choice of these parameters used to obtained the results shown in this proceeding are $\ell_{max}^{CMB} = \ell_{max}^{\psi} = 4096$.

5 Lensed CMB power spectra

In Figure 1 we show the comparison between the expected CMB lensed temperature C_ℓ^{TT} and the lensed B-modes of polarization power spectra C_ℓ^{BB} computed using CAMB, and the spectra extracted from our lensed CMB maps. For both these cases the simulated power spectra follow precisely the analytical signal. After having subtracted the shot-noise induced lensing contribution, the fractional difference between CAMB and the N-Body lensed spectra shows no significant bias up to $\ell \approx 3000$ where we start seeing effects due to the choice of ℓ_{max}^{CMB}. The latter is not high enough to properly resolve power on those scales with high-accuracy. The abrupt decrease in power observed on those scales for the ML approach w.r.t. the Born approximation is due to the effect of polynomial interpolation employed in Lenspix. As the latter tends to smooth the underlying signal, the consecutive application effectively removes more power on small angular scale with respect to the Born approach, for which the interpolation is performed only once. Similar results are obtained for the E-modes power spectrum. The situation however is different for the B-modes of polarization where we found the shot-noise contribution to be important at the percent level at small angular scales. This is expected given that B-modes are very sensitive to non-linear power, which is affected by shot-noise for $\ell >> 2000$.

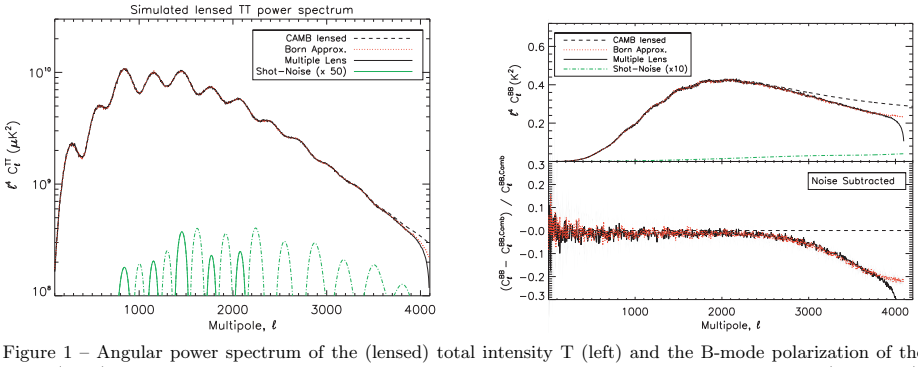

Figure 1 – Angular power spectrum of the (lensed) total intensity T (left) and the B-mode polarization of the CMB (right) compared to the theoretical expectation obtained with the Boltzmann code CAMB (black line). Red dotted line show results obtained in the Born approximation, while for the blue solid line the CMB is lensed through ML method. Green lines in both panels show the shot-noise contribution in the N-body simulation to the lensed spectra; green, dot-dashed lines represent the absolute value of this contribution.

[b] At this step we take into account the incidence angle of the light ray on the lens plane.

The lack of power due to the choice of ℓ_{max}^{CMB} starts to be important on angular scales larger than the ones affected in T and E-modes power spectra. This can be explained considering that at those scales a non-negligible fraction of the contribution to the BB power spectrum starts to come from progressively higher multipoles of both E and ψ that are not included by construction in the setup of our simulation [2,1].

6 CMB lensing jacobian simulation

Recent analytical work [4] claimed that large corrections at small angular scales are expected in the angular power spectrum of CMB lensing potential with respect to the results obtained with the Born approximation. The authors also made the hypothesis that the resolution of numerical simulations implemented in Calabrese et al.[1] were not sufficient to resolve these corrections. Motivated by these arguments, we expanded and improved the previous ray-tracing algorithm to explore and characterize the component of the full CMB lensing jacobian using the ML method [7,8] up to arc-minute scales. In this regime in fact non-linear effects are at most noticeable and beyond the limit of the results presented in the previous section. For this work we used the DEMNUni simulation [6] to produced 62 lens planes. To test these effects at the greatest level of accuracy we improved the raytracing method adopting the LenS^{2}HAT code [2] instead of LensPix. Thanks to its low memory footprint and massively parallelism we were able to propagate the full lensing jacobian together with the CMB light rays at a resolution of roughly 2arcsec over the full sky. In fig. 2 we show the power spectra of the CMB lensing observables extracted from its lensing jacobian at $z = 0$. We recover with high accuracy the consistency relation that exists between the lensing observables [8] while we see an excess of power in $\kappa, \epsilon$and E-mode of the α field with respect to the CAMB result due to the improved modeling of non-linearity and shot noise contribution of the N-body simulation. We also recover a purely second order non-zero ω, β field showing that the method is precise enough to resolve beyond Born corrections. We tested the convergence of the result as a function of the sky pixelization resolution and found it to be of the order of 0.5% for κ and ω fields. We also tested the stability of the result with respect to the number of lensing planes employed in the raytracing. A thinner slicing of the light-cone in shells of $50h^{-1}$Mpc (corresponding to an increase by a factor 3 in number of planes) lead to sub-percent differences in κ a 1% increase in ω.

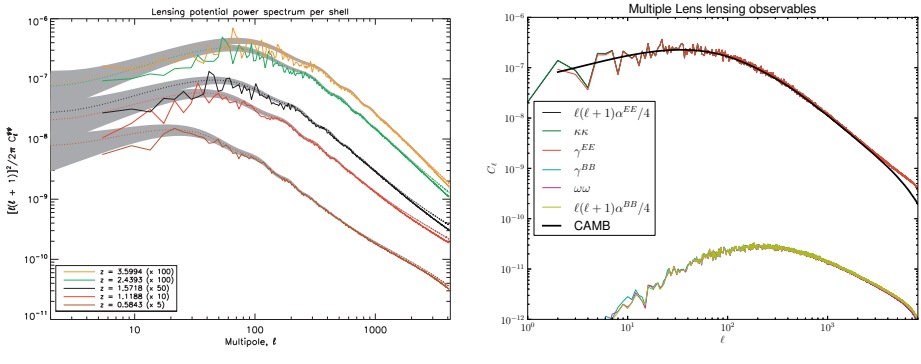

Figure 2 – Left: comparison between the angular power spectrum of the lensing potential computed with our algorithm from the CoDECS simulations (solid lines) and the analytical results in the Limber approximation at different redshifts. The grey area displays the cosmic variance. Right: convergence ($\kappa\kappa$), shear E (γ^{EE}) and B-modes (γ^{BB}) and rotation ($\omega\omega$) angular power spectra for CMB lensing. E and B-modes of the effective photon displacement $\alpha^{E/B}$ have been converted into the power spectra of the effective scalar potentials (see eq. 4).

References

1. Calabrese, M., Carbone, C., Fabbian, G., Baldi, M., & Baccigalupi, C. 2015, *JCAP* , 3, 049
2. Fabbian, G., & Stompor, R. 2013, *A & A*, 556, A109
3. Das, S., & Bode, P. 2008, *Astrophysical Journal*, 682, 1-13
4. Hagstotz, S., Schäfer, B. M., & Merkel, P. M. 2015, *MNRAS* , 454, 831
5. Baldi, M. 2012, *MNRAS* , 422, 1028
6. Castorina, E., Carbone, C., Bel, J., Sefusatti, E., & Dolag, K. 2015, *JCAP* , 7, 043
7. Hilbert, S., Hartlap, J., White, S. D. M., & Schneider, P. 2009, *A & A*, 499, 31
8. Becker, M. R. 2013, *MNRAS* , 435, 115
9. Das, S., & Ostriker, J. P. 2006, *Astrophysical Journal*, 645, 1